Altered Intestinal Microbial Flora and Abnormal Metabolism in Chinese Patients With Idiopathic Membranous Nephropathy

Xiaohu Shi
Peking Union Medical College Hospital
Zhaojun Li
Institute of Material Medical: Chinese Academy of Medical Sciences & Peking Union Medical College Institute of Materia Medica
Weifeng Lin
Peking University Third Hospital
Rongrong Hu
Peking Union Medical College Hospital
Gang Chen
Peking Union Medical College Hospital
Xuemei Li
Peking Union Medical College Hospital
Xuewang Lee
Peking Union Medical College Hospital
Sen Zhang (zhangs@imm.ac.cn)
Chinese Academy of Medical Sciences and Peking Union Medical College Institute of Materia Medica
https://orcid.org/0000-0003-1409-5795

Research

Keywords: Intestinal microbiome, Metabolites, Idiopathic membranous nephropathy

Posted Date: October 20th, 2021

DOI: https://doi.org/10.21203/rs.3.rs-961658/v1

Abstract

Background: Dysbiosis of the intestinal microbiome and related metabolites have been observed in chronic kidney disease (CKD), yet their roles in idiopathic membranous nephropathy (IMN) is poorly understood.

Results: In this study, we describe the variation of intestinal bacteria and fecal metabolites in patients with IMN for the first time in Chinese population. Stool samples are collected from 41 IMN patients at the beginning of diagnosis confirmation and 41 gender and age matched healthy control (HC). Microbial communities are investigated by sequencing of 16S rRNA genes and functional profiles predicted using Tax4Fun, and the correlation between intestinal bacteria and IMN clinical characteristics is also analyzed. Untargeted metabolomic analysis is performed to explore the relationship between colon's microbiota and fecal metabolites. IMN gastrointestinal microbiota demonstrates lower richness and diversity compared to HC, and exhibits a marked taxonomic and inferred functional dysbiosis when compared to HC. Some genera are closely related to the clinical parameters, such as Citrobacter and Akkermansia. 20 characteristic microbial biomarkers are selected to establish a disease prediction model with a diagnostic accuracy of 93.53%. Fecal metabolomics shows that tryptophan metabolism is reduced in IMN patients but uremic toxin accumulation in feces is not noticeable. Fecal microbiota transplantation demonstrates that gut dysbiosis impairs gut permeability in microbiota-depleted mice and induces NOD-like receptor activation in kidneys.

Conclusions: Clarifying the changes in intestinal microbiota in IMN patients will help further know the pathogenesis of this disease, and microbiota-targeted biomarkers will provide a potentially powerful tool for diagnosing and treating IMN.

1 Introduction

Membranous nephropathy (MN) is an autoimmune-mediated glomerular disease, and albuminuria is its most typical clinical manifestation, accompany by immune complex deposit in glomerular area by pathological test [1]. MN is the one of most common causes of nephrotic syndrome in adults, and 75% of MN cases have traditionally been designated as primary or "idiopathic" MN (IMN), and circulating autoantibodies directed against the M-type phospholipase A2 receptor (PLA2R1) was considered as major pathogenesis and biomarker of IMN [2]. Although IMN may spontaneously remit without treatment, as many as one third of patients have progressive loss of kidney function and may progress into chronic kidney disease (CKD), even to end-stage renal disease (ESRD) at a median of 5 years after diagnosis [3]. The ESRD incidence varies between 20% and 37% in most cases [4, 5], whereas 1% -7% in children [5]. Clinical heterogeneity suggests that IMN has complicated pathogenesis, but how the immune dysregulation is triggered and exact pathobionts of IMN are still not clear.

The gut microbiota plays an important role in shaping systemic immune response [6], and recently more and more evidences suggest that dysbiosis of intestinal flora is linked with chronic kidney disease (CKD),

and intestinal microbiota appears to be one of key factors in mediating the onset of kidney disease [7]. Meijers et al and Pahl et al put forward "gut-kidney axis" theory to explain the interaction between the kidney and intestinal flora [8]. According to this theory, intestinal microbiota disorders lead to accumulates of enterogenous urinary toxins in the gut [9–11], and the destruction of intestinal epithelial barrier causes the transfer of enterogenous urinary toxins and conditional pathogens into the blood circulation which can activate the intestinal mucosal immune system and induce a systemic microinflammatory response [12, 13], possibly leads to CKD. A series of CKD-related intestinal microbiota have been identified, and provide potential biomarkers or targets for further diagnosis and treatment for CKD [7, 14]. However, so far, based on our knowledge, there is not yet studies focusing on IMN, to investigate the alteration of intestinal microbiota in IMN patients. In the published studies about gut microbiota for CKD, patients used in 16s rRNA sequencing or shotgun metagenome sequencing are from mixed CKD cases with different pathogenesis, including diabetic nephropathy, lupus nephropathy, and several other glomerulonephritis [15, 16]. Although cohorts from these studies include MN subjects, the MN number are less, and do not differentiate IMN cases and secondary MN. Therefore, understanding distinguished intestinal microbiota dysbiosis in IMN patients is necessary, and also can provide evidence to explain the IMN pathogenesis from intestinal microbiota perspective.

In the current study, 41 IMN cases and matched 41 healthy control subjects have been enrolled into case-control cohort and circulating PLA2R1 antibody is used as IMN diagnosis biomarker to distinguish IMN from secondary MN. 16s rRNA sequencing is used to analyze intestinal bacterial changes in IMN patients, and the correlation between intestinal microbiota and clinical characteristics was further analyzed. Further to understand modified metabolic activity of the altered gut microbiome, untargeted metabolomics using UPLC–HDMS was performed to identify the differential metabolites between IMN and healthy control, which might be one of major contributors to the development and progression of IMN through network of microbiome-metabolomics. Finally, answering causal relationship between pathogenesis of IMN and microbiota dysbiosis, the feces from IMN patients and healthy control had been transplanted into germ-depleted mice to investigate the possible causal relationship between pathogenesis of IMN and microbiota dysbiosis.

Because geographic origin had a greater impact on the composition of the gut microbiota, all the IMN patients in the present study are from capital of China, Beijing. Heathy volunteers same from Beijing serve as controls to minimize variation caused by geographic influence. The other advantage of present study is that the feces were collected at the first diagnosis for patients, which avoided the modulated diet influence to gut biota because patients will adjust the diet once they know they have albuminuria, consequently change the intestinal microbiota to mock the real dysbiosis induced by IMN pathogenic factors.

2 Materials And Methods

2.1 Study cohort

All clinical studies are conducted with the subject informed and volunteered, and the study protocol was approved by the Ethics Committee of Peking Union Medical College Hospital and Peking University Third Hospital. A total of 82 subjects from Peking union medical college hospital and Peking University Third hospital were enrolled, including 41 IMN patients and same number of corresponding healthy controls from May 2019 to October 2019. All IMN patients eligible for this study were accurately diagnosed with following criteria: massive albuminuria (>3.0g/d), hypoalbuminemia (<25g/d), edema, hyperlipidemia, predominant IgG and C3 deposition in glomerular basement membrane by immunofluorescence, and positive for serum PLA2R1 autoantibody. Exclusive criteria for patients were as follows: (1) Patients with complicated diseases, acute and chronic infections, and habitual constipation; (2) Patients with chronic inflammatory bowel disease and coeliac disease; (3) Patients who received antibiotics, immunosuppressants, and functional foods (probiotics) within three months. The healthy controls possess the following characteristics: (1) with normal renal function and no kidney diseases, coeliac disease, habitual constipation and other complications; (2) did not received antibiotics, immunosuppressants and functional foods (probiotics) within three months. The age of all participants varies between 18-70 years old. The two groups were matched in age and gender, and they all lived in Beijing, capital of China. Fresh feces were immediately placed in sterile tubes and stored at -80°C.

Clinical data were collected through standard laboratory examination. Each subject's weight and height were measured, and the body mass index (BMI) was calculated. IMN clinical characteristics, such as blood urea nitrogen (BUN), serum creatinine (Scr), hematuria, proteinuria, 24-hour urinary protein, serum total cholesterol (TC), serum low-density lipoprotein cholesterol (LDL-C), serum high-density lipoprotein cholesterol (HDL-C), as well as the immunological indices including serum concentration of complement component C3 and C4, immunoglobulins IgA, IgG and IgM. Hematuria was quantified by dipstick analysis, and proteinuria by the sulphosalicylic acid method Creatinine clearance rate (CCr) was estimated by widely accepted formula described in previous publication [17]. The other clinical characteristics, such as blood pressure, hemoglobin and peripheral blood counting, covering neutrophils, lymphocytes and white blood cell (WBC) were also examined. In addition, serum concentration of PLA2R was tested as a biomarker for IMN.

2.2. Microbiome sample collection and DNA extraction

Fresh feces from all participants were placed in a fecal collection container, transported on ice, and stored at -80°. Bristol stool scale (a visual scale of the aspect of stool, from hard [1] to liquid [7]) was determined [18].Total genome DNA from samples was extracted using CTAB/SDS method. DNA concentration and purity were monitored on 1% agarose gels. According to the concentration, DNA was diluted to 1ng/μL using sterile water and stored at -20°C until further processing.

2.3 Bacterial 16S rRNA sequencing and data processing

All the sequencing and data processing were conducted by Novogene Co. Ltd (Beijing, China). Briefly, V3-V4 variable regions of 16S rRNA genes was amplified with universal primers 515F and 806R [19]. The amplicons were sequenced on an Illumina Miseq platform to obtain 300-bp paired-end reads. Paired-end

reads were then preprocessed using Trimmomatic software to detect and cut off ambiguous bases (N) [20]. It also cut off low quality sequences with average quality score below 20 using sliding window trimming approach. After trimming, paired-end reads were assembled using FLASH software [21]. Parameters of assembly were: 10bp of minimal overlapping, 200bp of maximum overlapping and 20% of maximum mismatch rate. Sequences were performed further denoising as follows: reads with ambiguous, homologous sequences or below 200bp were abandoned. Reads with 75% of bases above Q20 were retained. Then reads with chimera were detected and removed. These two steps were achieved using QIIME software (version 1.8.0) [22]. Clean reads were subjected to primer sequences removal and clustering to generate operational taxonomic units (OTUs) using Vsearch software with 97% similarity cutoff [23]. The representative read of each OTU was selected using QIIME package. All representative reads were annotated and blasted against Silva database Version 123 (16s rDNA) using RDP classifier (confidence threshold was 70%) [24]. Specific procedures for sequencing and analysis are described in Methods in the Supplemental Data.

According to the OTUs clustering results, taxomic annotation was made for the representative sequence of each OUT, and also obtain their abundance distribution. At the same time, abundance, alpha diversity calculation, Venn diagram and petal diagram were analyzed on OTUs to obtain richness and evenness information, common and unique OTUs among different groups, etc. Through dimensionality reduction analysis such as principal co-ordinates analysis (PCoA), community structure differences among different groups were explored. To further find out the community structure differences among the two groups, statistical methods such as t-test, MetaStat, LDA effect size (LEfSe) and Anosim were used for identifying significantly differential taxonomic composition. The annotation results of the amplicon were correlated with the corresponding functional database, and Tax4Fun software was used for functional prediction and analysis of the microbial community in the ecological samples.

2.4. Random forest model prediction

Considering the robustness of the algorithm, random forest provided in the R package random Forest was used to build the prediction model to identify the potential diagnostic biomarkers. The 16S rRNA abundance profiles were collected in the work, and the core genera in HC or IMN groups were filtered as prediction input variables. The important genera contributed to prediction were identified via a nested 10-fold cross-validation procedure. The area under curve (AUC) index and receiver operating characteristic (ROC) analysis were used to predicate the efficiency of possible cutoff values of the tests.

2.5. Sample preparation and UPLC–MS analysis for metabolomics

Faecal metabolites were performed using an untargeted metabolomics liquid chromatography-high-definition mass spectrometry (UPLC–HDMS). The metabolomic procedure, including sample preparation, metabolite separation and detection, data preprocessing and statistical analysis for metabolite identification, was performed following published protocols with minor modifications [25, 26]. Different statistical methods were applied to mine features that could distinguish IMN patients and healthy control.

We used partial least squares discriminant analysis (PLS-DA) and orthogonal partial least squares discriminant analysis (OPLS-DA) to evaluate the difference in metabolic profiles between HC and IMN patients [27]. The analysis was performed using the ropls version 1.12.0 (http://bioconductor.org/packages/release/bioc/html/ropls.html). All the observed and predicated compounds also were imported KEGG database. The significant metabolites with variable important in projection (VIP) ≥1, P value (T test) <0.05, and >2-fold changes were selected for further analysis.

2.6. Correlation analysis of genera and metabolites

To determine the association between gut microbiota and metabolites in IMN patients, we constructed a correlation analysis between gut microbiota and differential metabolites using Spearman's correlations in R version 3.4.3 (Hmisc package). The top 48 genera between two groups, and metabolites with >2-fold changes between IMN and HC, VIP≥1, P < 0.05 (T test) were analyzed.

2.7. Fecal bacterial cell counts and viability test

To determine the total, intact, and damaged bacterial cell count, flow cytometric analysis was performed on the fecal suspension supernatant (Supplementary Methods). Feces were 1000 times diluted with filtered phosphate-buffered saline, intact/damaged stained, and incubated for 13 minutes at 37℃ (Supplementary Methods). Samples were incubated using LIVE/DEAD® Bac Light™ Bacterial Viability Kits (Molecular Probes, Invitrogen, CA, USA) were analyzed with a four-laser BD FACSVerse flow cytometer (Becton Dickinson, San Jose, CA), equipped with a flow sensor for volumetric counting as previously described [28].

2.8. Fecal microbiota transplantation (FMT)

Fecal microbiota transplantation was performed according to the modified method described previously [29]. Briefly, 6-8-week-old male C57BL/6 mice received antibiotics (vancomycin, 50 mg kg− 1; neomycin sulfate 100 mg kg− 1; metronidazole 100 mg kg− 1; and ampicillin 50mg kg− 1) intragastrically once each day for 1 week to deplete the gut microbiota (Pseudo germ-free mice). The depletion efficiency was measured by counting the bacterium colonies in streak culture using faeces from animals described by previous studies [29]. FMT started one day after cessation of antibiotics, and total three groups were involved, which received saline (FMT-saline), feces from healthy control (FMT-Healthy) and faeces from IMN patients (FMT-IMN) respectively (N=6). Six normal mice without antibiotics treatment and FMT were used as normal control. Fecal samples were resuspended in sterile saline at 0.125 g/ml. The feces were ground with a 40μm sieve. The grinding solution was centrifuged at 800g for 3mins to remove the dregs. The sterile 1.2% sodium bicarbonate solution was orally administrated ahead of time to protect fecal microbes from gastric acid damage, then an amount of 0.2ml of the fecal solution was administered to mice in the corresponding groups orally via gastric gavage. The FMT procedure was shown in Supplemental Fig. S3A), and FMT was performed for total six times. All the mice were maintained on a germ-free condition with regular water and diet. After 17 days of first FMT, the urine and blood from each animal were collected for biochemical examination, meanwhile the kidneys and colorectal tissues were

harvested for pathological analysis and molecular research. Serum endotoxin level was measured by using a Pierce LAL Chromogenic Endotoxin Quantitation Kit (Thermo Scientific).

2.9. Histopathological analysis and immunohistochemistry

The kidney and colorectal tissues were harvested from FMT mice, and fixed into the 4% paraformaldehyde solution. The HE staining was performed for observing the histopathological damages. Immunohistochemistry with IL-6, IL-17, TNFα, NGAL and F4/80 was performed to evaluate the inflammatory status of kidney tissues and colorectal tissues. The immunohistochemistry protocol was described by previous studies from our laboratory [30, 31].

2.10. Gene expression profiling and quantitative PCR validation

The fresh kidney tissues were isolated immediately after animal sacrifice, and total RNA was extracted from 300 mg of renal epithelial tissue with the RNeasy Micro kit (Qiagen) following the manufacturer's protocol. Total RNA was quantified by NanoDrop ND-2000 (Thermo Scientific, Waltham, MA, USA) and RNA integrity was evaluated using the Agilent 2100 Bioanalyzer (Agilent Technologies, Santa Clara, CA, USA). The samples with RNA Integrity Number (RIN) ≥ 7 were subjected to the subsequent analysis. After removal of ribosomal RNA and then constructing a library, a high-throughput RNA sequencing was performed by Berry Genomics Ltd (Beijing, China). Mean fold-change in gene transcript levels between each two groups were calculated, and genes whose fold-change was over 1.5 were inputted into The Database for Annotation, Visualization and Integrated Discovery (DAVID) v6.7 for pathway analysis.

Aims to confirm the gene sequencing accuracy, cDNA was synthesized using High Capacity cDNA Reverse Transcription Kit (Applied Biosystems), and gene expression was measured by real-time qRT-PCR using specific primers/probes (Roche Universal Probe library, Table S7). PCR was performed using 7300 Real Time PCR machine (Applied Biosystems). The results are expressed as fold-change, and normalized to GAPDH expression.

2.11. Statistic analysis

The SPSS (ver. 21.0, SPSS Inc., Chicago, IL, USA) and R software (ver. 3.1.0, the R Project for Statistical Computing) were used for the statistical analysis. All the Effective tags in samples were clustered using Uparse software (Uparse v7.0.1001, http://www.drive5.com/uparse/)[32]; Mothur method and SILVA132 (SSUrRNA database) (http://www.arb-silva.de/) were used for taxonomic annotation analysis[33, 34]. α diversity was analyzed using Qiime software (Version 1.9.1), WGCNA, stats and gplot2 and vegan software packages were used for analyzing β diversity. The associations between genera with a prevalence > 1% and clinical parameters of IMN and healthy groups were evaluated using a generalized linear model (GLM) based on Spearman's correlation. MetaStat analysis was used to identify differential abundance taxa between two groups [35]. LEfSe (LDA Effect Size)[36] analysis was performed to find the microbial biomarker between groups by Kruskal-Wallis (KW) and rank test. Receiver operating

characteristic (ROC) curve was plotted to compare the prediction ability of selected metabolites and was built in “R” with “pROC” package (with a suitable threshold).

3 Results

3.1. The basic characteristics of study subjects

The general clinical and demographic data of IMN patients and healthy controls were summarized in **Table 1**. There were no significant differences in age, gender, bristol stool scale, fecal dry weight percentage between the two groups, but BMI in IMN group was significantly higher than healthy control, suggesting that obesity might be a risk factor for IMN pathogenesis. Compared with the healthy group, IMN patients have significantly higher levels in BUN, TC, LDL-C and peripheral neutrophil count, and lower hemoglobin and CCr ($P<0.05$). Remarkably proteinuria and hematuria were also observed in the urine of IMN patients. In addition, IMN patients have higher blood pressure compared with healthy control, which was indicated by significantly higher systolic blood pressure (SBP) and diastolic blood pressure (DBP) ($P<0.01$). Generally, CKD patients were categorized into five stages according to eGFR, using the Chronic Kidney Disease Epidemiology Collaboration (CKD-EPI)–creatinine equation, as recommended by the KDOQI, and all the cases in the current study belonged to stage 1 to stage 3.

3.2. Gut microbiome characteristics between IMN and healthy group

All the effective tags in samples were clustered in OTUs with 97% identity, and a total of 2061 OTUs were identified, 1183 OTUs were shared between two groups, with 252 OTUs specific in IMN group and 626 OTUs unique in healthy control (Fig.1A and supplemental table 1).

Richness of microbial communities between IMN and healthy control was evaluated by index of observed species, chao1 and ACE, which was shown in Fig.1B. Results showed that richness of intestinal microbiota in IMN group was significantly reduced compared with healthy control. α-diversity indexes of IMN group were also significantly lower than those of the healthy group, including shannon, simpson, phylogenetic diversity (PD) whole tree (Fig.1B). As for β-diversity, significant difference was also found based on the weighted (quantitative, ANOSIM $R=0.223$, $P=0.001$) but not unweighted (qualitative, $P > 0.05$) UniFrac between IMN and healthy groups (Fig. 1C), which indicated that presence of OTUs was not significantly different between two groups, but composition ratio of OTUs was more significantly different between IMN and healthy group. The relative abundance of taxa at different levels from microbiota between these two groups was shown in supplemental Fig.S1.

3.3. Differential taxa in intestinal microbiota between IMN and healthy groups

To best of our knowledge, it is the first description of gut dysbiosis in IMN patients from Chinese population, therefore, it is necessary to describe all the differential taxa at all the levels, including phylum, class, order, family and genus (supplemental table S2). On the phylum level, the Firmicutes/Bacteroidetes (F/B) ratio is considered as an important indicator in the composition of the intestinal microbiota, and as

shown Fig. 2A, the F/B ratio significantly increased in the IMN group compared with healthy control. In detail, Bacteroidetes in IMN group reduced significantly compared with healthy control (32.06% vs 18.91%, Healthy vs. IMN, P<0.01), and relative abundance of Firmicutes kept at almost same level between two groups (Fig.2B). MetaStat was used to analyze the significantly differential taxa at all the levels between two groups, and at the phylum level, besides of Firmicutes and Bacteroidetes, the Proteobacteria and Actinobacteria were enriched in IMN groups (P<0.05), and the minor phylum, Euryarchaeota was enriched in HC group (P<0.05). At the genus level, the bacteria detected in the IMN groups predominantly belonged to the *Bacteroides* (13.37%), *Bifidobacterium* (8.92%), *unidentified_Enterobacteriaceae* (7.52%), *Romboutsia* (5.29%), and *Faecalibacterium* (5.26%) genera. Likewise, the most abundant genus in the healthy group were *Bacteroides* (23.59%), followed by *Faecalibacterium* (9.69%), *Dialister* (3.32%), and *Bifidobacterium* (3.19%). As shown in Fig.3C, the top12 genera with most significant differences were following, *Romboutsia, unidentified Enterobacteriaceae, Bifidobacterium, Collinsella, unidentified Clostridiales, Citrobacter* were remarkably higher in IMN group (p<0.05), and *Bacteroides, Faecalibacterium, Dialister, Roseburia, Alistipes, Paraprevotella* were at higher level in the healthy group (p<0.05). The top 12 significant differential taxa at class, order and family were shown in supplemental Fig.S2.

Linear discriminant analysis (LDA) effect size (LefSe), a supervised learning model, was used to reduce the dimensions and identify the presence and effect size of specific taxa between IMN and healthy group. A logarithmic LDA score cutoff of 4.0 was set up in the current study, and total 22 taxa at all levels were discovered as high-dimensional fecal microbiota biomarkers between IMN and healthy groups (LDA score (log_{10})>4, p<0.05) (Fig.3A and 3B). At phylum level, Proteobacteria and Actinobacteria significant increased in IMN group, while Bacteroidetes increased in healthy group. At class level, IMN group showed higher enrichment of Gammaproteobacteria and unidentified Actinobacteria, while Bacteroidia were significantly enriched in healthy group. At order level, Enterobacterial and Bifidobacterial were higher in IMN group, whereas Bacteroidia increased in healthy group. At family level, IMN group was characterized by higher abundance of Enterobacteriaceae, Bifidobacteriaceae and Peptostreptococcaceae, whereas normal group was characterized by Bacteroidaceae and Ruminococcaceae. At genus level, IMN patients were mainly characterized by higher relative abundance of *unidentified Enterobacteria, Bifidobacterium, Romboutsia, whereas the relative abundance of the genera Dialister, Faecalibacterium, Bacteroides* were higher in healthy samples. At species level, *Escherichia coli* was in higher abundance in IMN group, while *Bacteroides dorei* was more enriched in healthy group.

GLMs were used to model the genera that were significantly different between IMN and healthy subjects after controlling for possible confounding factors, such as age, gender and BMI. The differences between feces from IMN and healthy control were associated with the genera *Bifidobacterium, unidentified Enterobacteriaceae, Romboutsia, Collinsella, Citrobacter, unidentified Clostridiales, Lactobacillus, Blautia, Intestinibacter, Haemophilus, Dorea, Fusicatenibacter* (p<0.05, table 2), suggesting that these genera were associated with IMN. On the other hand, genera *Alistipes, Roseburia, Paraprevotella, Butyricicoccus,*

Barnesiella, Dialister, Bacteroides, Faecalibacterium, Sutterella were negatively associated with IMN (P<0.05, table 2).

3.4. IMN-related microbiota biomarker predictive model

In order to screen the representative taxa at genus level as biomarkers to distinguish IMN efficiently and specifically from healthy persons, random forest model (RF) was used to build a predictive model based on fecal microbiota profile using the significantly different abundance genera from MetaStat test as the input. Here, 20 genera predicted IMN are screened out through Mean Decrease Accuracy and Mean Decrease Gini using the RF model (Fig.3C). The diagnosis performance of these 20 genera combination was evaluated by receiver operating characteristic curve (ROC). The AUC (the area under the receiver operating characteristic curve) was 93.53%, with confidence interval (CI):0.8775-0.9931 (Fig.3D).

3.5. Associations of the gut microbiome with clinical indicators

We carried out the correlation analysis between gut microbiota (genus level, at a prevalence>1%) and IMN clinical parameters, which were related with systemic immune status, abnormal lipid metabolism and renal function respectively (Fig.4). For indicators related to systemic immune status, *Dialister* had the significant positive correlation with serum C3(sC3), sC4 and sIgM, meanwhile *Faecalibacterium* was only positively related to sC3 (p<0.05) and *Fusicatenibacter* was positively correlated with sIgG (p<0.01). Genus *Phascolarctobacterium* and *unidentified Prevotellaceae* had a significant negative correlation with sIgA (P<0.05 and P<0.01 respectively). As for renal function indicators, the genera *Terrisporobacter*, *Intestinibacter*, *Citrobacter*, *Streptococcus, unidentified Clostridiales, Klebsiella* and *unidentified Ruminococcaceae* were all positively associated with hematuria (p<0.01 in unidentified Ruminococcaceae). Among them, *unidentified Clostridiales* and *Klebsiella* also had a positive correlation with 24h proteinuria (p<0.01 and p<0.05 respectively). In addition, *Fusobacterium* was negatively associated with BUN (p<0.05). *Streptococcus* had a positive correlation (p<0.05) while *Parabacteroides* and *Akkermansia* had a negative correlation with glomerular IgG deposition (p<0.05 and p<0.01 respectively). Regard to parameters related to blood pressure and lipid metabolism, *Collinsella* had a significant negative association with SBP and DPB, while *Bifidobacterium* only showed the negative correlation with DBP. Besides, we could observe that *unidentified Prevotellaceae, unidentified Clostridiales* and *Citrobacter* were all positively correlated with total serum cholesterol (P<0.01). Similarly, *Dialister, unidentified Clostridiales* and *Sutterella* were positively associated with TG (p<0.01 in Dialister). As for HDL, genera *Parabacteroides, Flavonifractor, Bacteroides, Alistipes, Roseburia* and *Akkermansia* displayed the remarkable positive correlation (p<0.01), while *Streptococcus* and *Lactobacillus* showed the significant negative relationship (p<0.05). Beyond these, *unidentified Enterobacteriaceae* had a significant positive association with LDL (p<0.05), while *Fusobacterium* was negatively correlated with LDL (p<0.05).

In addition, we could discover that some genera were associated with peripheral WBC, neutrophils, lymphocytes and hemoglobin (HGB), which were related to innate immunity and human basically physical condition. *Lactobacillus* was negatively related to WBC and neutrophils (p<0.05), while *Alistipes*

showed the positive correlation with neutrophils ($p<0.05$). *Unidentified Enterobacteriaceae* and *Dialister* had positive relevance with peripheral lymphocyte number ($p<0.05$). Anemia is common complication for kidney disease, and for HGB, genus *unidentified Prevotellaceae, Phascolarctobacterium, Flavonifractor, Bacteroides* and *Parabacteroides* displayed remarkable negative correlation ($p<0.01$), whereas *Collinsella, Dorea* and *Haemophilus* were positively correlated with HGB ($p<0.05$).

Short-chain fatty acids (SCFA) producing bacteria were considered to be protective for CKD, and we compared their relative abundance between two groups, and analyzed their correlation with clinical parameters, including *Roseburia, Faecalibacterium, Clostridium* and *Paraprevotella*. *Roseburia,* although decreased 50% in IMN group compared with healthy control, it did not show correlation with any clinical characters in the current study. *Faecalibacterium* also decreased in IMN group (9.7% in healthy group vs. 5.3% in IMN), and its abundance was positively with serum C3. *Clostridium* did not change between two groups. *Paraprevotella* decreased from 0.53% (healthy group) to 0.06% (IMN), but no significant correlation with clinical parameters was found.

Although serum PLA2R antibody was a biomarker for IMN, no specific genus which had significant correlation with serum PLA2R antibody was found among all the differential genera.

3.6. Function prediction analysis

Tax4Fun was used to predict the functions of the differential intestinal microbiota of two groups, based on functional annotation information of OTUs using the Silva database sequence as a reference. According to the annotation results of Kyoto Encyclopedia of Genes and Genomes (KEGG) pathway database, abundant of functional groups - KOs (KEGG orthologous groups) had been screened, and a total of 6508 KOs were identified from IMN and healthy groups, of which 1587 KOs were identified with significantly different abundance between two groups (false discovery rate (FDR), $P<0.05$), illustrating that there were functional aspects of the gut microbiota associated with IMN. All the significantly differential KOs were listed in Table S3, and top 26 KOs based on difference significance were shown in Fig.5A. The predictive microbiota functions at level 1 and 2 KEGG pathways were shown in Fig.5B. Among them, genetic information processing, replication and repair, membrane transport, translation, nucleotide metabolism, cellular community-prokaryotes were highly enriched in IMN samples ($p<0.01$), whereas gene function that related carbohydrate metabolism, energy metabolism, glycan biosynthesis and metabolism and catabolism were higher in healthy group, $p<0.01$.

Total 390 level 3 KEGG pathways had been identified by OTU annotation in two groups. By calculating FDR-corrected P value <0.05, 158 significantly differential KEGG pathways were identified between two groups based on OUT abundance on pathways, which was shown in Fig.5C. Top five enriched pathways in IMN group were transporters, DNA repair and recombination protein, phenylalanine tyrosine and tryptophan biosynthesis, purine metabolism and pyrimidine metabolism ($P<0.01$), whereas amino sugar and nucleotide sugar metabolism, pyruvate metabolism, alanine-asparate-glutamate metabolism, butanoate metabolism were significantly up-regulated in healthy groups ($P<0.01$).

3.7. Fecal metabolite profiles

To confirm the alteration of function of gut microbiota, we explored the metabolic profile in the same fecal samples as that of 16s rDNA sequencing using an untargeted approach, through liquid chromatography-mass spectrometry and examined the relationship between microbiota and metabolites. A total of 2340 metabolites were identified. Heatmap and volcano analysis based on criteria (P<0.05, VIP>1 and fold change >2) identified total 466 differential fecal organic compounds, and 112 up and 354 down in IMN patients compared with healthy control, which was shown in Fig.6A and 6B and supplemental table S4. We observed a clear discrimination on fecal concentrations of their gut bacterial fermentation metabolites between these two groups both on PCA and PLS-DA score analysis (Fig.6C and 6D), reflecting the modified metabolic activity of the altered gut microbiome. The differential metabolites were classified into most abundant 15 chemical categories which was shown in Fig.6E, and top three are “amino acid, peptide and analogues”, “purine and purine derivates” and “fatty acid and conjugates”. Aims to understand the changed metabolism pathways due to gut microbiota dysbiosis, KEGG enrichment was performed with all significantly differential metabolites, however, only caffeine metabolism pathway emerged with P=0.002, Fatty acid biosynthesis (P=0.081), Vitamin digestion and absorption (P=0.089), and Oxidative phosphorylation (P=0.090), and other pathways all had P value higher than 0.1 (Fig.6F).

To explore the potential relationships between the gut microbiome changes and metabolic products, a correlation matrix was generated using Spearman correlation, and only top ten genera enriched in IMN and correlation with statistical difference were shown in Fig.6G. All the abundance of *Bifidobacterium, Fusicatenibacter,* and *Lactobacillus* positively correlated with the level of threitol, myricetin, dUMP, toltrazuril, geranylgeranyl pyrophosphate, xylitol, tanespimycin, and 3-[2-(2-pyridyl)ethyl]-1H-indole, and their correlation coefficient was higher than 0.7. *Intestinibacter* and *Citrobacter* shared similar metabolic pattern and positively correlated with Sulfaquinoxaline, Esculetin, Hydroxypyruvic acid and 2-Hydroxyestradiol. L-Arginine was positively correlated with *Romboutsia* with coefficient was 0.92. Whether these compounds play roles in IMN occurrence and progression deserves further clarification. The detailed correlation coefficients and significances between all the differential genera and all the differential metabolites (fold change>2, P<0.05, and VIP>1) were provided in supplemental table S5 and S6.

Aromatic amino acid, tyrosine, phenylalanine and tryptophan, and their metabolites in the intestine, contribute to the resource of main uremic toxins [37]. In the present research, as shown in table 3, only tryptophan significantly increased in IMN feces sample compared with healthy control (20% increased, P<0.01), which was partly consistent with enhanced tryptophan biosynthesis pathway in gut microbiota of IMN group (Fig.5C). Indole, one of tryptophan uremic toxin metabolite precursor, significantly decreased almost half in IMN group (P=0.002), which was explained that that tryptophan accumulation in the faeces of IMN patients. Another endogenous tryptophan metabolite 5-methoxytryptophan, was reported to be one of most promising biomarker metabolites for detection of early-stage CKD in serum, decreased in the feces of IMN (P<0.05), which was consistent with previous report [38]. Other tryptophan metabolites, such as 5-Methoxytryptamine, skatole, 3-Indoleacrylic acid were all significantly decreased in

IMN group. Meanwhile, 3-indoxyl sulfate was higher in IMN group without statistical significance. We speculated that higher 3-indoxyl sulfate might contribute from plasma accumulation, instead of bacterium metabolism. tyrosine, phenylalanine and their uremic metabolite, p-cresol, did not change significantly between IMN and healthy group (table 3). The other well-known gut microbiota derived uremic toxin, trimethylamine N-oxide (TMAO), was also not altered between two groups (table 3).

3.8. Fecal bacterial cell counts and viability test before FMT

Antibiotic mixture can clear more than 90% of bacteria from the intestine, which were confirmed by counting the bacterium colonies in streak culture using faeces from animals (Supplemental Fig. S3B). The color of feces in antibiotics-treated animals seemed to be darker than before treatment (Supplemental Fig. S3C). The fecal bacterial cell counts and intactness in human samples were examined by flow cytometry, and the number of intact and damaged bacterial cells did not differ between IMN and healthy control, and about 90% bacteria are intact and live bacteria (Supplemental Fig. S3D). We calculated the live number of bacteria per gram of human feces, to make sure that same number of live bacteria was transfected into pseudo germ-free mice.

3.9. FMT affected renal function and lipid metabolism in mice

Four days after final FMT, blood and urine of mice were collected for laboratory examination. It could be found in Fig.7A that the levels of BUN and Scr in the FMT-IMN group was significantly higher than FMT-healthy group ($P<0.01$), but not different from FMT-saline group. The serum albumin levels were not different among three groups (Fig.7A). As for the lipid metabolism parameters, the serum LDL were significantly increased in FMT-IMN group compared with the FMT-healthy group ($P<0.05$), but not serum TG and total CHO (Fig.7A). As for the urinary indexes, the ratio of microalbumin/creatinine, NAG/creatinine and NGAL/creatinine were all significantly elevated in FMT-IMN group compared with other groups, which suggested that more renal serious injuries had been caused by FMT with IMN faeces (Fig.7B). Further HE staining showed that there were more glomerular hyperplasia and enlargement of tubular lumen in FMT-IMN group than FMT-healthy group. Immunohistochemistry using IgG indicated that more IgG immune complex was deposited in glomeruli of FMT-IMN group, and immunohistochemistry using NGAL also demonstrated that renal local inflammation and tubular slight injury in FMT-IMN group was aggravated than FMT-healthy group (Fig.7C).

Antibiotics treatment could cause body weight loss compared with normal control, and this loss was gradually reverse after terminating antibiotics. As shown in Fig. 7D, the growth curve of body weight in the FMT-healthy group and FMT-IMN group were both higher than that in the FMT-saline group, suggesting that intestinal flora has the function of providing nutrition. Body weight of FMT-IMN groups was slightly higher than FMT-healthy group, and also consistent with that BMI index in IMN patients was higher than healthy control.

3.10. Intestinal inflammation, endotoxin and NOD-like receptor activation contribute to the aggravated kidney injury by IMN-FMT

Aims to understand the molecular mechanisms of FMT with IMN feces aggravating kidney injuries, the mRNA sequencing was performed using total mRNA from kidney tissue in each group. Differential genes between FMT-IMN and FMT-healthy groups were mainly enriched in the following pathways by KEGG analysis (Fig.8A): Cytokine-cytokine receptor interaction, TNF signaling pathways, chemokine signaling pathways, and NOD-like receptor signaling pathways, and these pathways were all associated with inflammation. Specifically, the cytokine receptor interaction pathway mainly enriched the following genes: CCL12, CXCL2, CCL7, CCL5, IL9R and CCL20; GM5431, CCL12, CXCL2, CCL20 and CCL5 was mainly enriched in TNF signaling pathway; CCL12, CXCL2, CCL7, ADCY2, CCL5 and CCL20 were mainly enriched in the chemokine signaling pathway; and MEFV, CXCL2, CCL12, LCN2 and CCL5 were mainly enriched in NOD like receptor signaling pathway. The expression levels of the above genes in each group were further confirmed by QRT-PCR, and it could be found that the expression levels of these cytokines in the kidney tissues from FMT-IMN group were significantly higher than those from the FMT-healthy and FMT-saline groups (Fig.8B). Besides that, the “intestinal immune network for IgA production” and “systemic lupus erythematosus” pathways were also upregulated in FMT-IMN group, and activation of these pathways also contributed to the pathophysiology of IMN (Fig.8A).

NOD-like receptor pathway was most enriched pathway in KEGG analysis, which suggested that pathogens, like bacteria and endotoxin, might translocate into the systemic circulation through the impaired intestinal mucosal permeability. Elevated serum LPS level (Fig.8C) and more damaged structural integrity of intestinal tissue (Fig.8D) in FMT-IMN group confirmed this speculation. Immunohistochemistry further demonstrated higher expression of pro-inflammation cytokines and macrophage infiltration into the colon tissues of FMT-IMN group than the FMT-healthy group (Fig.8E).

4. Discussion

IMN is an autoimmune glomerulonephritis, which can progress into CKD. Although several studies have reported that intestinal dysbiosis plays an important role in CKD[14] and autoimmunity disease [39], there is no investigation focusing on IMN so far. Understanding of intestinal microbiota composition and alteration is a basis for utility of human gut microbiota in the diagnosis and treatment [40], and our study clarified taxonomic changes and composition of intestinal microbiota in the Chinese IMN patients for the first time. The strength of our study lies in a relatively comprehensive description of microbial communities associated with IMN, and the utilization of prediction models to identify differentially bacterial taxa in the disease, as well as correlation study with IMN clinical characteristics. The recruitment of patients and healthy control from one city is another important advantage that may largely mitigate the influence of geographic distribution on the diversity of intestinal microbiota. Besides that, the most striking merit of current study is that it is probably the first report that 12 genera associated with IMN pathogenesis have been identified by GLM in a case-control study.

The Firmicutes/Bacteroidetes ratio is considered as an important factor in the composition of the intestinal microbiota and increase of this ratio is considered to increases susceptibility to several physiological activities, infections, immune disorders, inflammation, oxidative stress and insulin

resistance [41, 42]. In the present study, the F/B ratio is higher in IMN patients compared with healthy control group, and higher F/B ratio is mostly due to lower relative abundance of Bacteroidetes. In the previous study of gut microbiota with CKD in Chinese population, Li et al report that F/B ratio does not change in CKD patients [43], and by analyzing their demographic data, we find in that study, the BMI in CKD patients is not different from healthy control. However, in our study, the IMN patients has significantly higher BMI than healthy control, we postulate that is the possible reason why F/B ratio is higher in our study, which also suggests that obesity might be potential risk for IMN pathogenesis. The F/B ratio increased in IMN patients also suggest the possible chronic inflammation status in human body[44]. However, Maria De Angelis reported that in the IgA nephropathy from Italian cohort study, even under same BMI index, the IgA patients has lower abundance of Bacteroidetes and unchanged Firmicutes, which is consistent with our results[45], which suggests that lower Bacteroidetes is a potential risk factor for IMN.

IMN is an autoimmune disease, therefore it is necessary to compare with some autoimmune diseases. In here, we compared with three systemic lupus erythematosus (SLE) cohort studies from Spain and China, and F/B ratio is reduced in two studies, and one is not changed, which is not compatible with IMN, which suggest IMN has the unique gut dysbiosis different from SLE [46]. One study using 45 Chinese SLE patients suggest that abundance of a number of bacterial genera such as *Rhodococcus, Eubacterium, Flavonifractor, Eggerthella, Klebsiella*, and *Prevotella* was significantly higher, while abundance of *Pseudobutyrivibrio* and *Dialister* was lower in SLE patients [39]; compared with IMN subjects in our study, only *Rhodococcus, Eggerthella* and *Dialister* have the same trend as SLE, other genera are not different compared with healthy group.

Both β-diversity and α-diversity significantly decrease in IMN groups compared with healthy control in the current study, which is consistent with most CKD studies[43], as well as IgA nephritis[45]. However, the reduction is more statistically significant compared to other studies [47]. The possible explanation is that subjects in current study are all unique IMN patients instead of combination of heterogenous CKD patients. There is another phenomenon which is not consistent with previous studies, that is β-diversity is not significant in unweighted univariance analysis, but at weighted Univariance. The possible reason is that IMN is auto-immunity disease, its pathogenesis mostly relies on internal physiological change instead of outside environment factors or introduction of new genera from outside environment. Taken together, both α-diversity and β-diversity indexes provide solid evidences that the intestinal microbiota in IMN is different from that of healthy subjects.

LEfSe analysis is a high-dimensional biomarker discovery and interpretation used to identify and describe the differential genomic characteristics between two or more biological conditions[36]. In the present study, LEfSe was applied to altered microbiota data from the two groups, identifying 22 differential taxonomic clades with an LDA score higher than 4.0. Through the random forest model and ROC analysis, we observed that 20 genera combination has a high diagnosis power which can distinguish IMN diseases well (AUC is 93.53%), therefore, these findings may lead to the development of bioassays with prognostic value for the risk of IMN, also these are useful biomarkers for diagnosis.

Tax4Fun is used for functional analysis which is based on SILVA database that updated every month. However, there are still some limitations in predicting the function using 16S rRNA, and metagenomic sequencing may be more accurate in predicting the gene function of bacteria. Tax4fun predicted differential 158 KEGG pathways between two groups, almost 40% in total predicted 390 KEGG pathway, which suggest that IMN has significant different changes in biofunction of intestinal microbiota. At level 2, purine metabolism significantly increased in IMN group, and uric acid, as a purine metabolic end product, might increase with enhanced purine metabolism, and consequently impair the intestinal barrier [48]. In addition, Transporter is one of most enriched KEGG pathway in IMN, may suggest intestinal tight junction was impaired and more renal toxins might be transported into circulating blood via leaking intestinal barriers.

Identification of disease-specific bacterium genera and clarifying its relationship with disease pathogenesis is an important way to understand the role of intestinal microbiota. For example, Cheol Kwak et al demonstrate that there is an inverse correlation between intestinal *Oxalobacter formigenes* and urinary oxalate levels in patients with calcium oxalate urolithiasis, and supports the concept that *O. formigenes* is necessary in maintaining oxalate homeostasis and lack of enteric O. formigenes is a risk factor of urolithiasis[49]. In our results, MetaState analysis provides valuable information about abundant differential bacteria at different levels, further by spearman correlation analysis with clinical parameters, several genera were found be significantly correlated with clinical parameters, such as TG, sC3, sC4, sIgA, sIgG, BUN, proteinuria, HGB, HDL and LDL, suggesting that these genera may play important roles in IMN pathogenesis. These findings provide genus candidates for further study how these bacteria initiate or aggravate IMN, and may provide new targets for IMN diagnosis and treatment. Following I will discuss several important genera which are potential in IMN pathogenesis.

Genus *Lactobacillus* belongs to Lactic acid bacteria, generally are considered to be beneficial microorganisms and have been associated with multiple potential health effects in both humans and animals [50]. However, a study from Egypt find the *Lactobacillus* is significantly higher in CKD patients than healthy control, and moreover, the *Lactobacillus* is higher in CKD with cardiovascular disease (CVD) than CKD without CVD, suggesting *Lactobacillus* could not provide renal protective effect [51]. The current study showed that the average abundance of *lactobacillus* is almost five times higher in IMN group than healthy control, consistent with study from Egypt, and GLM analysis also suggest it is pathogen for IMN. Meanwhile, *Lactobacillus* is negatively correlated with HDL-C, which was beneficial for cardiovascular disease, also shows its worsening role in lipid metabolism dysregulation. However, its abundance also negatively correlated with peripheral neutrophil counting, which means *Lactobacillus* has a certain effect on lowering systemic inflammatory stress in IMN group. This controversy effect for *lactobacillus* in IMN needs function test using *in vivo* study.

Hypertension is one of complications of IMN. From the clinical data in table 1, blood pressure is higher in IMN patients than healthy control. In the current study, *Bifidobacterium* and *Collinsella* were found to be negatively with blood pressure, but these two genera are enriched in IMN than healthy control, which was

also found in the other CKD cohorts[52]. Liu et al report *Bifidobacterium* is negative with blood pressure in Chinese hypertension population[53]. *Bifidobacterium* is an anaerobic gram-positive bacterium that is widely found in the human gastrointestinal tract, and accounts for 3-6% of adult feces[54, 55]. Most *Bifidobacteria* are pro-health that improve the immune system[56–59]. In the current study, although *Bifidobacteria* is enriched in IMN group, it is negative correlated with hypertension, which suggest that it might be protective in blood pressure control for IMN patients to some extent. Previous studies have shown that *Collinsella* is associated with obesity, atherosclerosis, and abnormal lipid metabolism[60–63]. GLM analysis suggest it is positive with IMN, but correlation study suggest it is negative with hypertension and positively with HGB, seemingly also partly beneficial in IMN. *Bifidobacterium* and *Collinsella* also showed controversy sign, which deserves further function study too.

Faecalibacterium decreased in IMN group (9.7% in healthy group vs. 5.3% in IMN), and its protective effect on IMN was also confirmed GLM analysis. *Faecalibacterium* is butyrate producing bacterium [37], and it is reasonable to postulate that the less butyrate produced by *Faecalibacterium* is also a risk factor for IMN. *Akkermansia* is considered as a next-generation star microbe because abundant of reports indicate that genus *Akkermansia*, especially *Akkermansia muciniphila*, benefit glucose metabolism, lipid metabolism, and intestinal immunity[64, 65], and enhance sensitivity to checkpoint blockade immunotherapy[66]. In the current study, the relative of abundance of *Akkermansia* is found to be positively with serum HDL-cholesterol concentration, and negative with the IgG deposition grades in glomeruli, which indicate that *Akkermansia* is also beneficial for IMN, and supplementation with *Akkermansia* is possible treatment strategy against IMN.

Microbially derived metabolites influence the host through multiple pathways. Increasing evidences show that some metabolic products of gut microbiota can enter the bloodstream and exert important influences on the physiology and behavior of the hosts[27]. CKD is characterized by accumulation of protein-bound uremic toxins such as pcresyl sulfate, p-cresyl glucuronide, indoxyl sulfate and indole-3-acetic acid, which originate in the gut. Intestinal bacteria metabolize aromatic amino acids into p-cresol and indole, (further conjugated in the colon mucosa and liver) and indole-3-acetic acid. [37]. There is increasing interest in the colonic microbiota as a relevant source of uremic retention solutes accumulating in CKD[67]. However, in the current study, when we screened these precursor and metabolites, surprisingly, no toxin precursors were found to be significantly increased compared with healthy control. On the contrary, indole significantly reduced in IMN group and tryptophan catabolism was inhibited. Our findings are comparable to the results of Tessa Gryp et al., who observed no difference in fecal p-cresol and indole levels among healthy control, hemodialysis patients and CKD patients [37], and plasma uric toxins retention is mainly caused by impaired kidney function instead of increased uremic toxin production by microbial dysbiosis. On the other hand, although indoxyl sulfate is a uremic toxin, the indole also plays several beneficial effects in host intestinal homeostasis. Both *in vitro* and *in vivo* studies have indicated that indole enhances intestinal epithelial barrier functions by increasing expression of genes involved in maintenance of epithelial cell structure and function[68, 69]. Besides indole,

other tryptophan catabolites, such as skatole 3-Indoleacrylic acid (decreased in IMN patients), also affect mucosal homeostasis by decreased intestinal permeability possibly mediated by the pregnane X receptor[70]. Therefore, reduction of tryptophan catabolism in gut microbiota may contribute to the susceptibility of IMN, especially possible for early stages (the IMN patients in current study are all between stage 1 to stage 3 kidney dysfunction)

Caffeine metabolism is the most significant KEGG pathway by IMN fecal metabolite enrichment analysis, and previous studies suggest that long-term caffeine consumption exacerbates renal failure in obese, diabetic, ZSF1 (fa-facp) rats, and caffeine potentiated the development of more severe tubulointerstitial changes and increased focal glomerulosclerosis[71, 72].

The current FMT study provides new pathophysiological insights into the causal relationship between gut microbiota dysbiosis and the IMN, opening a new venue of therapeutic strategy to treat IMN. Herein, we showed that IMN-associated microbial dysbiosis caused gut barrier dysfunction, abnormal elevation of circulating LPS, and enhancement of the renal inflammation via NOD-like receptor signaling pathway, leading to an increase in IMN susceptibility. One novel study shows that gut microbiota dysbiosis promotes age-related atrial fibrillation by lipopolysaccharide and glucose-induced activation of NOD-like receptor protein (NLRP)-3 inflammasome-inflammasome [73], which also provides evidence that NOD-like receptor pathway may be one of common pathways through which microbiota dysbiosis induce the diseases.

There are several limitations of the present study. One is all the subjects in the current study are from Chinese population, and there might be different in composition of intestinal microbiota from other countries. Second is that the sample size is not large, and more patients are needed to validate the results. Thirdly, 16s sequencing has limitations on species identification and function analysis, and shotgun metagenome analysis, which can provide more detailed information, is also needed to analyze fecal microbiota in IMN; the last limitation is that we did not collect the patient serum in parallel to investigate that dysregulation of fecal metabolites cause alteration of serum metabolites.

Conclusion

Taken together, gut microflora dysbiosis occurred in the occurrence and progression of IMN. Landscape of characteristics of intestinal microbiota in IMN patients was described for the first time in the current study. By GLM and correlation study of intestinal bacteria with clinical parameters, we found several bacteria closely related to IMN, which may help to understand the pathogenesis of IMN. These IMN associated microbiota may provide new targets for the early diagnosis and treatment for IMN.

Abbreviations

CKD, chronic kidney disease; IMN, idiopathic membranous nephropathy; HC, healthy control; PLA2R1, phospholipase A2 receptor; ESRD, end-stage renal disease; BMI, body mass index; BUN, blood urea

nitrogen; Scr, serum creatinine; TC, total cholesterol; LDL-C, low-density lipoprotein cholesterol; HDL-C, high-density lipoprotein cholesterol; CCr, Creatinine clearance rate; WBC, white blood cell; OTUs, operational taxonomic units; PCoA, principal co-ordinates analysis; LEfSe, LDA effect size; AUC, area under curve; ROC, receiver operating characteristic; UPLC–HDMS, untargeted metabolomics liquid chromatography-high-definition mass spectrometry; PLS-DA, partial least squares discriminant analysis; OPLS-DA, orthogonal partial least squares discriminant analysis; VIP, variable important in projection; FMT, Fecal microbiota transplantation; CKD-EPI, Chronic Kidney Disease Epidemiology Collaboration.

Declarations

Ethical Approval and Consent to participate

All clinical studies are conducted with the subject informed and volunteered. All subjects agreed using their samples and data. The study protocol was approved by the Ethics Committee of Peking Union Medical College Hospital and Peking University Third Hospital (Approval number: ZS-2455).

Consent for publication

Written informed consent for publication was obtained from all participants.

Availability of data and materials

The datasets used or analyzed during the current study are available from the corresponding author on reasonable request.

Competing interests

The authors declare that there were no conflicts of interest in the study.

Funding

We appreciate the funding from Chinese academy of medical sciences Innovation Fund for Medical Sciences (CIFMS, NO.2017-I2M-1-009; NO. 2016-I2M-3-011), “Drug Innovation Major Project of China” (2018ZX09711001-002-010), and Beijing Natural Science Foundation (7202138, 7181007).

Authors' contributions

XHS and SZ were responsible for the conception and design of the study. ZJL, WFL and RRH were responsible for acquisition and analysis of data; GC, XML and XWL conducted statistical analysis and results analysis. SZ drafted the manuscript

Acknowledgments

None.

Authors' information

Prof. Sen Zhang, Ph.D.

State Key Laboratory of Bioactive Substances and Functions of Natural Medicines, Institute of Materia Medica, Chinese Academy of Medical Sciences & Peking Union Medical College, Beijing 100050, PR China

References

1. Couser WG. Primary Membranous Nephropathy. Clinical journal of the American Society of Nephrology: CJASN. 2017;12:983–97.
2. Ma H, Sandor DG, Beck LH. Jr. **The role of complement in membranous nephropathy**. Semin Nephrol. 2013;33:531–42.
3. McGrogan A, Franssen CF, de Vries CS. **The incidence of primary glomerulonephritis worldwide**: **a systematic review of the literature**. *Nephrology, dialysis, transplantation: official publication of the European Dialysis and Transplant Association - European Renal Association* 2011; 26: 414-430.
4. Cattran DC, Brenchley PE. Membranous nephropathy: integrating basic science into improved clinical management. Kidney international. 2017;91:566–74.
5. Ronco P, Debiec H. Pathophysiological advances in membranous nephropathy: time for a shift in patient's care. Lancet. 2015;385:1983–92.
6. Sivan A, Corrales L, Hubert N, et al. Commensal Bifidobacterium promotes antitumor immunity and facilitates anti-PD-L1 efficacy. Science. 2015;350:1084–9.
7. Anders HJ, Andersen K, Stecher B. The intestinal microbiota, a leaky gut, and abnormal immunity in kidney disease. Kidney Int. 2013;83:1010–6.
8. Meijers BK, Evenepoel P. **The gut-kidney axis**: **indoxyl sulfate**, **p-cresyl sulfate and CKD progression**. *Nephrology, dialysis, transplantation: official publication of the European Dialysis and Transplant Association - European Renal Association* 2011; 26: 759-761.
9. Di Iorio BR, Marzocco S, Nardone L, et al **Urea and impairment of the Gut-Kidney axis in Chronic Kidney Disease**. *Giornale italiano di nefrologia: organo ufficiale della Societa italiana di nefrologia* 2017; 34.
10. Nallu A, Sharma S, Ramezani A, et al. Gut microbiome in chronic kidney disease: challenges and opportunities. Translational research: the journal of laboratory clinical medicine. 2017;179:24–37.
11. Rossi M, Johnson DW, Campbell KL. The Kidney-Gut Axis: Implications for Nutrition Care. Journal of renal nutrition: the official journal of the Council on Renal Nutrition of the National Kidney Foundation. 2015;25:399–403.
12. Yang T, Richards EM, Pepine CJ, et al. The gut microbiota and the brain-gut-kidney axis in hypertension and chronic kidney disease. Nature reviews Nephrology. 2018;14:442–56.

13. Cigarran Guldris S, Gonzalez Parra E, Cases Amenos A. Gut microbiota in chronic kidney disease. Nefrologia. 2017;37:9–19.
14. Vaziri ND, Wong J, Pahl M, et al. Chronic kidney disease alters intestinal microbial flora. Kidney international. 2013;83:308–15.
15. Margiotta E, Miragoli F, Callegari ML, et al. Gut microbiota composition and frailty in elderly patients with Chronic Kidney Disease. PloS one. 2020;15:e0228530.
16. Meijers B, Evenepoel P, Anders HJ. Intestinal microbiome and fitness in kidney disease. Nat Rev Nephrol. 2019;15:531–45.
17. Nahler G. creatinine clearance (CCr). In: **In**: **Nahler G, editor.** *Dictionary of Pharmaceutical Medicine*. Springer Vienna: Vienna; 2009. pp. 42–2.
18. Lewis SJ, Heaton KW. Stool Form Scale as a Useful Guide to Intestinal Transit Time. Scand J Gastroenterol. 1997;32:920–4.
19. Nossa CW, Oberdorf WE, Yang L, et al. Design of 16S rRNA gene primers for 454 pyrosequencing of the human foregut microbiome. World journal of gastroenterology. 2010;16:4135–44.
20. Bolger AM, Lohse M, Usadel B. Trimmomatic: a flexible trimmer for Illumina sequence data. Bioinformatics. 2014;30:2114–20.
21. Reyon D, Tsai SQ, Khayter C, et al. FLASH assembly of TALENs for high-throughput genome editing. Nature biotechnology. 2012;30:460–5.
22. Caporaso JG, Kuczynski J, Stombaugh J, et al. QIIME allows analysis of high-throughput community sequencing data. Nature methods. 2010;7:335–6.
23. Edgar RC, Haas BJ, Clemente JC, et al. UCHIME improves sensitivity and speed of chimera detection. Bioinformatics. 2011;27:2194–200.
24. Wang Q, Garrity GM, Tiedje JM, et al. Naïve Bayesian Classifier for Rapid Assignment of rRNA Sequences into the New Bacterial Taxonomy. Appl Environ Microbiol. 2007;73:5261–7.
25. Ni J, Shen TD, Chen EZ, et al **A role for bacterial urease in gut dysbiosis and Crohn's disease**. *Sci Transl Med* 2017; 9.
26. Theriot CM, Koenigsknecht MJ, Carlson PE Jr., *et al.* Antibiotic-induced shifts in the mouse gut microbiome and metabolome increase susceptibility to Clostridium difficile infection. Nat Commun. 2014;5:3114.
27. Dan Z, Mao X, Liu Q, et al **Altered gut microbial profile is associated with abnormal metabolism activity of Autism Spectrum Disorder**. *Gut Microbes* 2020: 1–22.
28. Van Nevel S, Koetzsch S, Weilenmann H-U, et al. Routine bacterial analysis with automated flow cytometry. J Microbiol Methods. 2013;94:73–6.
29. Smirnova E, Puri P, Muthiah MD, et al. Fecal Microbiome Distinguishes Alcohol Consumption From Alcoholic Hepatitis But Does Not Discriminate Disease Severity. Hepatology. 2020;72:271–86.
30. Sen Z, Weida W, Jie M, et al. Coumarin glycosides from Hydrangea paniculata slow down the progression of diabetic nephropathy by targeting Nrf2 anti-oxidation and smad2/3-mediated

profibrosis. Phytomedicine. 2019;57:385–95.

31. Zhang S, Xin H, Li Y, *et al.* **Skimmin**, **a Coumarin from Hydrangea paniculata**, **Slows down the Progression of Membranous Glomerulonephritis by Anti-Inflammatory Effects and Inhibiting Immune Complex Deposition**. *Evid Based Complement Alternat Med* 2013; 2013: 819296.
32. Haas BJ, Gevers D, Earl AM, et al. Chimeric 16S rRNA sequence formation and detection in Sanger and 454-pyrosequenced PCR amplicons. Genome research. 2011;21:494–504.
33. Edgar RC. UPARSE: highly accurate OTU sequences from microbial amplicon reads. Nature methods. 2013;10:996–8.
34. Wang Q, Garrity GM, Tiedje JM, et al. Naive Bayesian classifier for rapid assignment of rRNA sequences into the new bacterial taxonomy. Appl Environ Microbiol. 2007;73:5261–7.
35. White JR, Nagarajan N, Pop M. S**tatistical methods for detecting differentially abundant features in clinical metagenomic samples**. PLoS Comput Biol. 2009;5:e1000352.
36. Segata N, Izard J, Waldron L, et al. Metagenomic **biomarker discovery and explanation**. Genome biology. 2011;12:R60.
37. Gryp T, De Paepe K, Vanholder R, et al. Gut microbiota generation of protein-bound uremic toxins and related metabolites is not altered at different stages of chronic kidney disease. Kidney Int. 2020;97:1230–42.
38. Chen DQ, Cao G, Chen H, et al. Identification of serum metabolites associating with chronic kidney disease progression and anti-fibrotic effect of 5-methoxytryptophan. Nat Commun. 2019;10:1476.
39. Mu Q, Zhang H, Liao X, et al. Control of lupus nephritis by changes of gut microbiota. Microbiome. 2017;5:73.
40. Khoury T, Tzukert K, Abel R, *et al.* **The gut-kidney axis in chronic renal failure**: **A new potential target for therapy**. *Hemodialysis international International Symposium on Home Hemodialysis* 2017; 21: 323-334.
41. Rinninella E, Raoul P, Cintoni M, et al **What is the Healthy Gut Microbiota Composition? A Changing Ecosystem across Age, Environment, Diet, and Diseases**. *Microorganisms* 2019; 7.
42. Méndez-Salazar EO, Ortiz-López MG, Granados-Silvestre, MdlÁ, et al **Altered Gut Microbiota and Compositional Changes in Firmicutes and Proteobacteria in Mexican Undernourished and Obese Children**. *Frontiers in Microbiology* 2018; 9.
43. Li F, Wang M, Wang J, et al **Alterations to the Gut Microbiota and Their Correlation With Inflammatory Factors in Chronic Kidney Disease**. *Frontiers in Cellular and Infection Microbiology* 2019; 9.
44. Sochocka M, Donskow-Łysoniewska K, Diniz BS, et al. The Gut Microbiome Alterations and Inflammation-Driven Pathogenesis of Alzheimer's Disease—a Critical Review. Mol Neurobiol. 2019;56:1841–51.
45. De Angelis M, Montemurno E, Piccolo M, et al. Microbiota and metabolome associated with immunoglobulin A nephropathy (IgAN). PloS one. 2014;9:e99006.

46. Rahbar Saadat Y, Hejazian M, Bastami M, et al. The role of microbiota in the pathogenesis of lupus: Dose it impact lupus nephritis? Pharmacol Res. 2019;139:191–8.
47. Jiang S, Xie S, Lv D, et al. Alteration of the gut microbiota in Chinese population with chronic kidney disease. Scientific reports. 2017;7:2870.
48. Ramezani A, Raj DS. The gut microbiome, kidney disease, and targeted interventions. J Am Soc Nephrol. 2014;25:657–70.
49. Kwak C, Kim HK, Kim EC, *et al.* **Urinary Oxalate Levels and the Enteric Bacterium Oxalobacter formigenes in Patients with Calcium Oxalate Urolithiasis**. *European Urology* 2003; 44: 475–481.
50. Ji X, Hou C, Zhang X, et al. Microbiome-metabolomic analysis of the impact of Zizyphus jujuba cv. Muzao polysaccharides consumption on colorectal cancer mice fecal microbiota and metabolites. Int J Biol Macromol. 2019;131:1067–76.
51. Mahmoud Okba A, Youssef Shahin R, Halim Baki A, et al **Role of intestinal microbiota in cardiovascular disease risk in end stage renal disease patients**. *QJM: An International Journal of Medicine* 2018; 111.
52. Mafra D, Borges N, Alvarenga L, *et al.* **Dietary Components That May Influence the Disturbed Gut Microbiota in Chronic Kidney Disease**. *Nutrients* 2019; 11.
53. Liu J, An N, Ma C, et al. Correlation analysis of intestinal flora with hypertension. Exp Ther Med. 2018;16:2325–30.
54. Saavedra JM. Use of probiotics in pediatrics: rationale, mechanisms of action, and practical aspects. Nutrition in clinical practice: official publication of the American Society for Parenteral Enteral Nutrition. 2007;22:351–65.
55. Lewis ZT, Totten SM, Smilowitz JT, et al. Maternal fucosyltransferase 2 status affects the gut bifidobacterial communities of breastfed infants. Microbiome. 2015;3:13.
56. Collado MC, Gueimonde M, Hernandez M, et al. Adhesion of selected Bifidobacterium strains to human intestinal mucus and the role of adhesion in enteropathogen exclusion. J Food Prot. 2005;68:2672–8.
57. Serafini F, Strati F, Ruas-Madiedo P, et al. Evaluation of adhesion properties and antibacterial activities of the infant gut commensal Bifidobacterium bifidum PRL2010. Anaerobe. 2013;21:9–17.
58. Round JL, Mazmanian SK. The gut microbiota shapes intestinal immune responses during health and disease. Nature reviews Immunology. 2009;9:313–23.
59. Nicola S, Amoruso A, Deidda F, *et al.* **Searching for the Perfect Homeostasis**: **Five Strains of Bifidobacterium longum From Centenarians Have a Similar Behavior in the Production of Cytokines**. *Journal of clinical gastroenterology* 2016; 50 Suppl 2, Proceedings from the 8th Probiotics, Prebiotics & New Foods for Microbiota and Human Health meeting held in Rome, Italy on September 13-15, 2015: S126-s130.
60. Astbury S, Atallah E, Vijay A, et al **Lower gut microbiome diversity and higher abundance of proinflammatory genus Collinsella are associated with biopsy-proven nonalcoholic steatohepatitis**. *Gut microbes* 2019: 1–12.

61. Gomez-Arango LF, Barrett HL, Wilkinson SA, et al. Low dietary fiber intake increases Collinsella abundance in the gut microbiota of overweight and obese pregnant women. Gut Microbes. 2018;9:189–201.
62. Kourosh A, Luna RA, Balderas M, et al. Fecal microbiome signatures are different in food-allergic children compared to siblings and healthy children. Pediatric allergy immunology: official publication of the European Society of Pediatric Allergy Immunology. 2018;29:545–54.
63. Karlsson FH, Fak F, Nookaew I, et al. Symptomatic atherosclerosis is associated with an altered gut metagenome. Nat Commun. 2012;3:1245.
64. Naito Y, Uchiyama K, Takagi T. A next-generation beneficial microbe: Akkermansia muciniphila. Journal of clinical biochemistry nutrition. 2018;63:33–5.
65. Zhang T, Li Q, Cheng L, et al. Akkermansia muciniphila is a promising probiotic. Microbial biotechnology. 2019;12:1109–25.
66. Ansaldo E, Slayden LC, Ching KL, et al. Akkermansia muciniphila induces intestinal adaptive immune responses during homeostasis. Science. 2019;364:1179–84.
67. Poesen R, Windey K, Neven E, et al. The Influence of CKD on Colonic Microbial Metabolism. J Am Soc Nephrol. 2016;27:1389–99.
68. Bansal T, Alaniz RC, Wood TK, et al. The bacterial signal indole increases epithelial-cell tight-junction resistance and attenuates indicators of inflammation. Proc Natl Acad Sci U S A. 2010;107:228–33.
69. Shimada Y, Kinoshita M, Harada K, et al. Commensal bacteria-dependent indole production enhances epithelial barrier function in the colon. PloS one. 2013;8:e80604.
70. Roager HM, Licht TR. Microbial tryptophan catabolites in health and disease. Nat Commun. 2018;9:3294.
71. Tofovic SP, Kost CK Jr, Jackson EK, et al. Long-term caffeine consumption exacerbates renal failure in obese, diabetic, ZSF1 (fa-fa(cp)) rats. Kidney Int. 2002;61:1433–44.
72. Tofovic SP, Salah EM, Jackson EK, et al. Early renal injury induced by caffeine consumption in obese, diabetic ZSF1 rats. Ren Fail. 2007;29:891–902.
73. Zhang Y, Zhang S, Li B, et al **Gut microbiota dysbiosis promotes age-related atrial fibrillation by lipopolysaccharide and glucose-induced activation of NLRP3-inflammasome**. *Cardiovasc Res* 2021.

Tables

Table1 Characteristics of the study subjects

Index	Healthy n=41	IMN n=41	P value
Age (year)	48±12	54±14	0.0579
Sex	M 25（61.0%）	M 25（61.0%）	1.00
	F 16（39.0%）	F 16（39.0%）	
BMI (kg/cm^2)	23.73±3.03	27.06±5.81	0.002
Scr (umol/L)	74.26±16.60	86.24±34.76	0.0564
Hematuria (+)	0	1.39±0.70	—
BUN(mmol/L)	4.51±1.04	6.38±2.84	0.0003
24h-UP(g/24h)	—	4.90±3.33	—
CCr (ml/min)	97.12±13.40	85.49±25.57	0.0089
SBP(mmHg)	117.12±15.49	132.17±16.82	0.000
DBP(mmHg)	74.10±13.11	81.39±10.40	0.007
TC(mmol/L)	5.03±0.91	6.81±1.93	0.000
TG (mmol/L)	1.81±2.69	2.69±1.75	0.0875
HDL-C(mmol/L)	1.39±0.37	1.30±0.41	0.2994
LDL-C(mmol/L)	3.12±0.86	4.08±1.59	0.0017
WBC(10^9/L)	5.58±1.16	8.22±3.34	0.0000
NEUT(10^9/L)	3.30±1.06	5.70±3.13	0.0000
LYM (10^9/L)	1.71±0.42	1.88±0.76	0.2381
HGB (g/L)	144±15.51	132±22.55	0.0073
PLT (10^9/L)	255.72±76.54	253.26±68.12	0.8811
PLA2R(EU/ml)	—	167.27±173.69	—
C3(g/L)	—	1.12±0.19	—
C4(g/L)	—	0.26±0.06	—
IgG(g/L)	—	6.40±2.86	—
IgA(g/L)	—	2.01±1.24	—
IgM(g/L)	—	0.95±0.54	—
Fecal parameters			

Bristol Stool Scale	4.0 (3.8–5.0)	4.5 (3.0–5.3)	0.0214
Dry weight (%)	0.27 ± 0.05	0.25±0.10	0.0845

M: Male, F, Female. Ccr: Creatinine clearance; 24h-UP: 24 hour urine protein;

Data which are normally distributed are shown as mean ± SD, and compared by student's t-test; data which are not normally distributed are shown as median (range, 25-75 percentile) and compared by non-parametric Kruskal-Wallis test. Sex distribution was analyzed by χ^2 test.

Table 2. GLMs for fecal genera based on differences between IMN and healthy control group

Study group	Genus	Coefficient	95% CI	P value
IMN vs. Healthy	Lactobacillus	1.166	0.461~1.875	<0.001
	Citrobacter	1.214	0.539~1.881	<0.001
	Bifidobacterium	1.070	0.500~1.635	<0.001
	unidentified_Enterobacteriaceae	1.675	1.139~2.207	<0.001
	Romboutsia	0.793	0.364~1.225	<0.001
	Collinsella	1.050	0.554~1.540	<0.001
	Blautia	0.306	0.011~0.602	0.0415
	Intestinibacter	0.618	0.015~1.222	0.0447
	Haemophilus	1.797	1.034~2.560	<0.001
	Dorea	0.244	0.001~0.488	0.0473
	Fusicatenibacter	0.531	0.198~0.865	0.0013
	unidentified_Clostridiales	0.648	0.183~1.121	0.0045
	Alistipes	-0.738	-1.302~-0.167	0.0065
	Roseburia	-0.487	-0.931~-0.042	0.0279
	Paraprevotella	-2.382	-3.079~-1.675	<0.001
	Butyricicoccus	-0.396	-0.652~-0.140	0.0029
	Barnesiella	-1.695	-2.295~-1.088	<0.001
	Dialister	-1.409	-2.043~-0.768	<0.001
	Bacteroides	-0.832	-1.235~-0.424	<0.001
	Faecalibacterium	-0.603	-0.925~-0.280	<0.001
	Sutterella	-1.161	-1.800~-0.511	<0.001

Result of the GLMs for significant genera (sequence counts) based on the group factors (IMN and healthy group) and possible confounding factors (age, gender and BMI) of 82 subjects.

The coeffienct value (positive number) indicated the taxa were associated with IMN patients.

GLM, general linear model; CI, confidence interval; BMI, body mass index.

Table 3. Differential uremic toxins in healthy control and IMN patients

metabolite	Fold change (IMN/Healthy)	P value
L-tyrosine	1.02	0.7
L-phenylalanine	1.14	0.7
DL-tryptophan	1.59	0.005
L-tryptophan	1.20	0.007
5-methoxytryptophan	0.80	0.001122109
p-cresol	2.67	0.93
Phenol	0.825	0.11
Indole	0.593	0.002
indole-3-acetic acid	1.49	0.5
5-Methoxytryptamine	0.435198509	0.000118635
Skatole	0.229787626	0.003527695
3-Indoleacrylic acid	0.794464353	0.073948886
3-indoxyl sulfate	3.43	0.25
Trimethylamine N-oxide	1.2	0.665

Figures

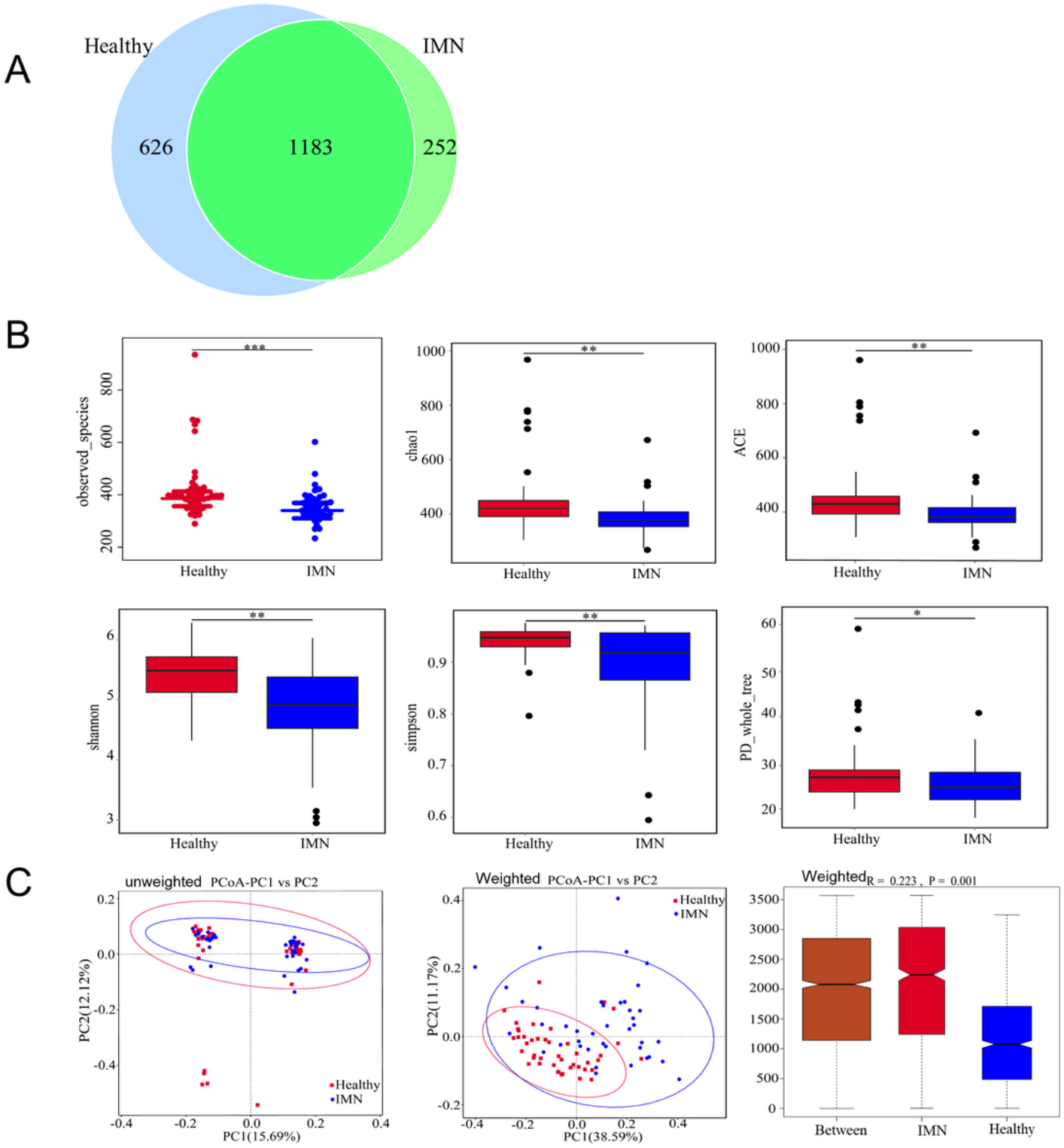

Figure 1

Alpha Diversity and Beta Diversity of gut microbiota between IMN and healthy groups. (A) Venn diagram of unique and shared OTUs between IMN and healthy group. (B)The microbiota richness index (observed species, chao1, ACE) and α-Diversity analysis index (shannon, Simpson, PD whole tree) of different samples based on OUT counts. (C) Unweighted and weighted ANOSIMs and PCOA based on the distance matrix of UniFrac dissimilarity of the fecal microbial communities in the IMN and healthy groups.

ANOSIM R values show the community variation between the compared groups, and significant P values are indicated. The axes represent the two dimensions explaining the greatest proportion of variance in the communities. *, P<0.05, **, P<0.01, ***, P<0.001.

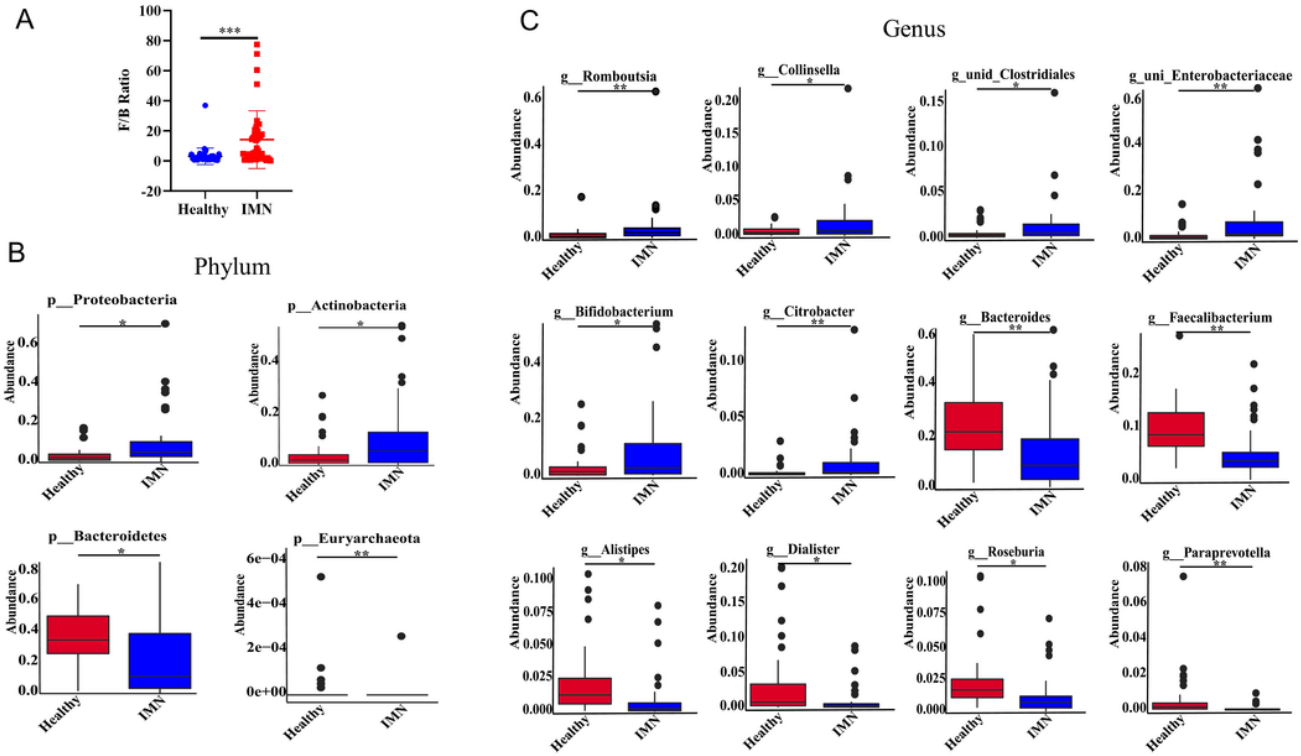

Figure 2

Differential taxa at different levels between IMN and healthy groups. MetaStat was used to screen microbiota with significant differences between groups at the genus level. The horizontal axis was the group, vertical axis is the relative abundance of corresponding taxa. A) F/B ration at phylum level between two groups; Differential taxa at phylum B) and genus C) levels between two groups. *P<0.05, **P<0.01.

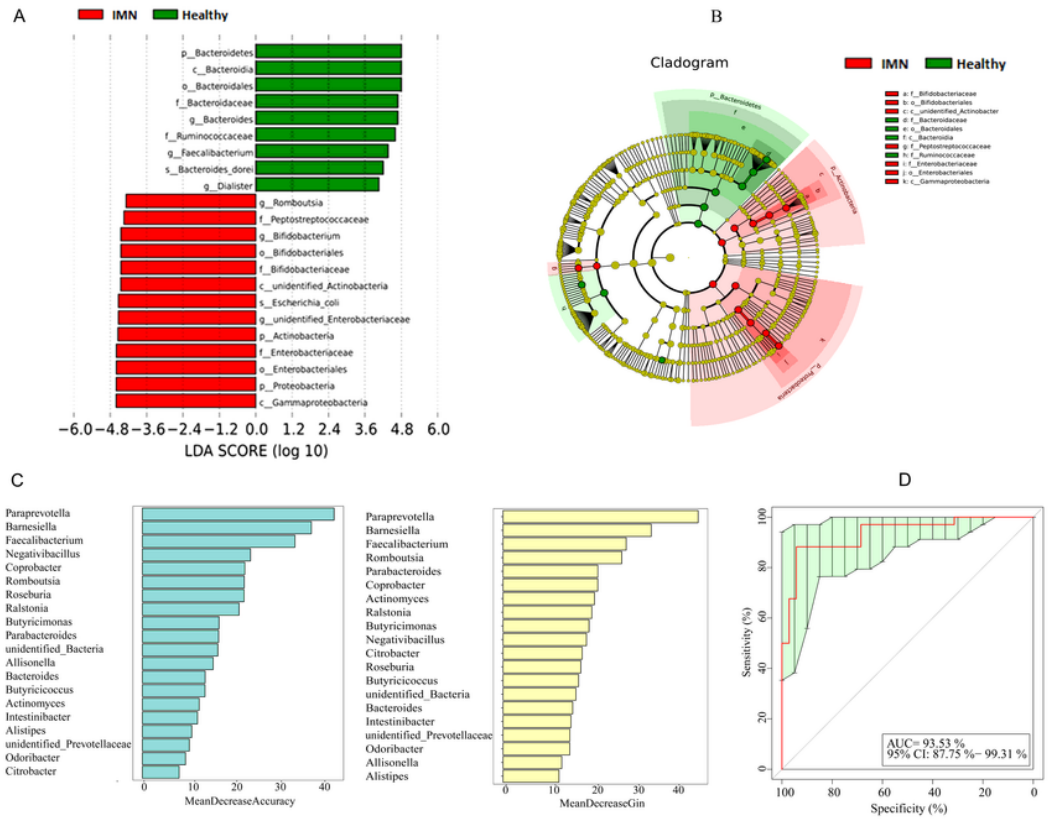

Figure 3

Important microbiota biomarker screening between IMN and healthy groups. (A)Linear Discriminant Analysis (LDA) Effect Size (LEfSe) analysis revealed biomarkers with significant difference between IMN and healthy groups using LDA histogram and cladogram. The LDA score >4 and p<0.05 were listed. (B) Cladogram using LEfSe method indicating the phylogenetic distribution of fecal microbiota associated with IMN and healthy subjects. (C)The predictive model based on genus level was made. The relatively important genus was screened using Mean Decrease Accuracy and Mean Decrease Gin (D) ROC curve generated by Random Forest model. The Area Under the Curve (AUC) was used as a strong indicator for the evaluation of the classification model. p, phylum; c, class; o, order; f. family; g, genus; RF, Random Forest; ROC, receiver operating characteristic; AUC, area under the ROC curve; CI, confidence interval.

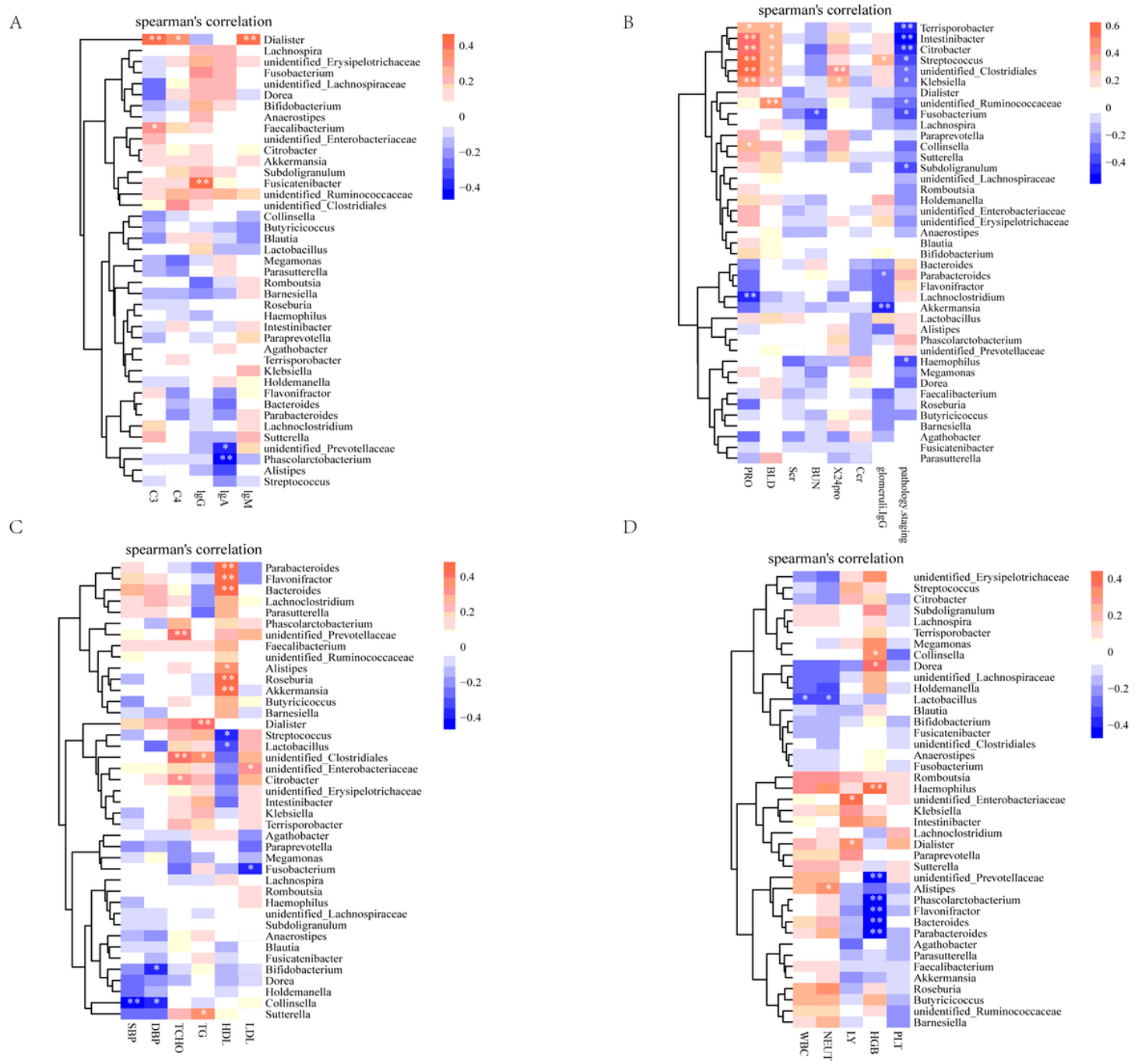

Figure 4

Heatmaps showing correlations between gut microbiota and IMN clinical parameters. The microbiota genera(prevalence>1%) were showed. The IMN clinical parameters are related to A) immune status, B) renal function, C) lipid metabolism, D) innate immunity. *p<0.05; **p<0.01. BLD: blood, refers to hematuria.

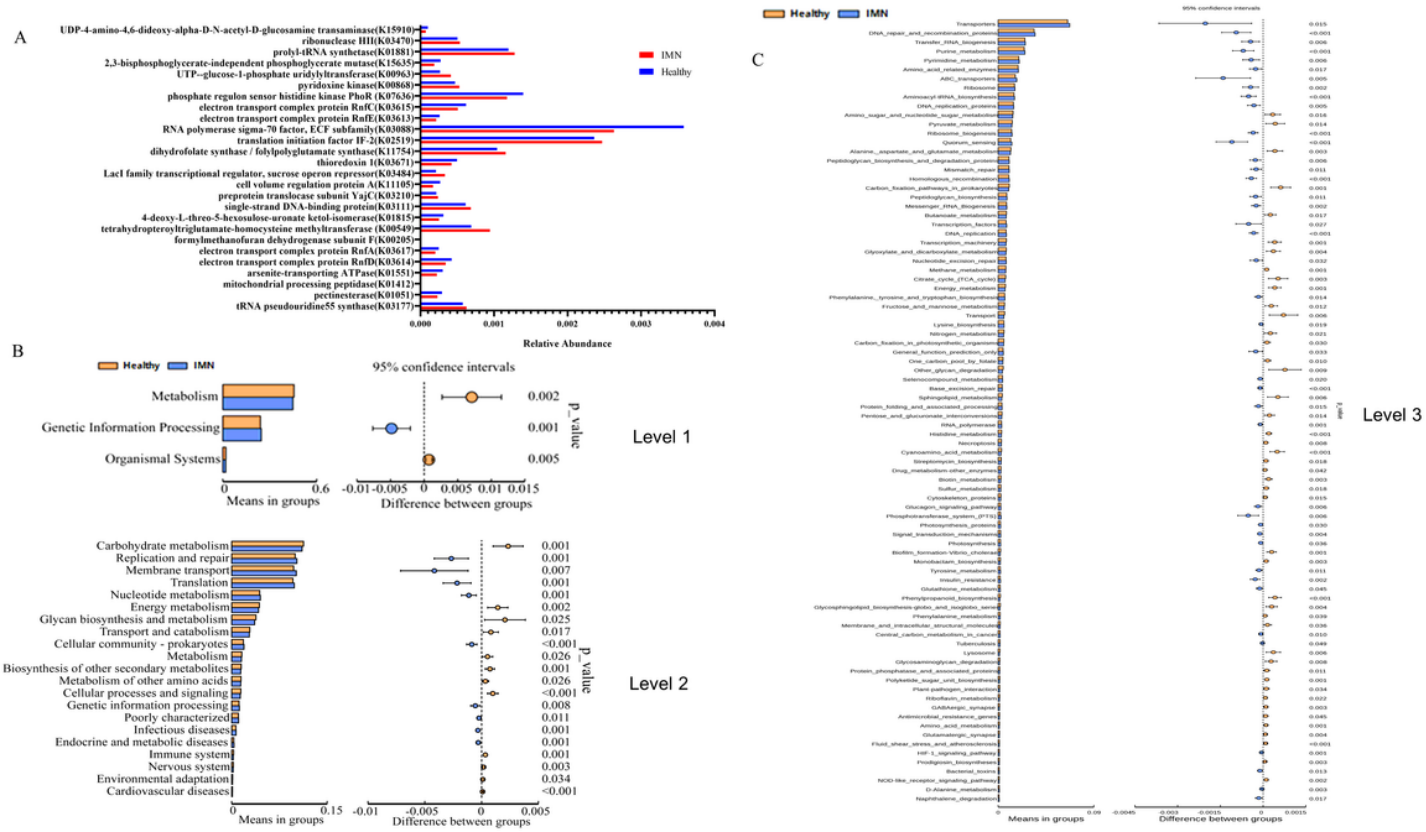

Figure 5

Functional predictions for the gut microbiota between IMN and healthy groups. (A)The KOs with significantly different abundance between IMN and healthy controls using Tax4Fun. (B,C) Significant KEGG pathways in different level for the gut microbiota between the IMN and healthy groups. In B and C, the left figure shows the differences in KEGG abundance between groups. Each bar represents the mean abundance of pathway with significant differences in each group. The right figure shows the confidence between groups. The left-most endpoint of each circle represents the lower limit of the 95% confidence interval of the mean difference, while the right-most endpoint represents the upper limit of the 95% confidence interval of the mean difference. The group represented by the color of the circle is the group with high mean value. At the far right end of the presentation is the p value.

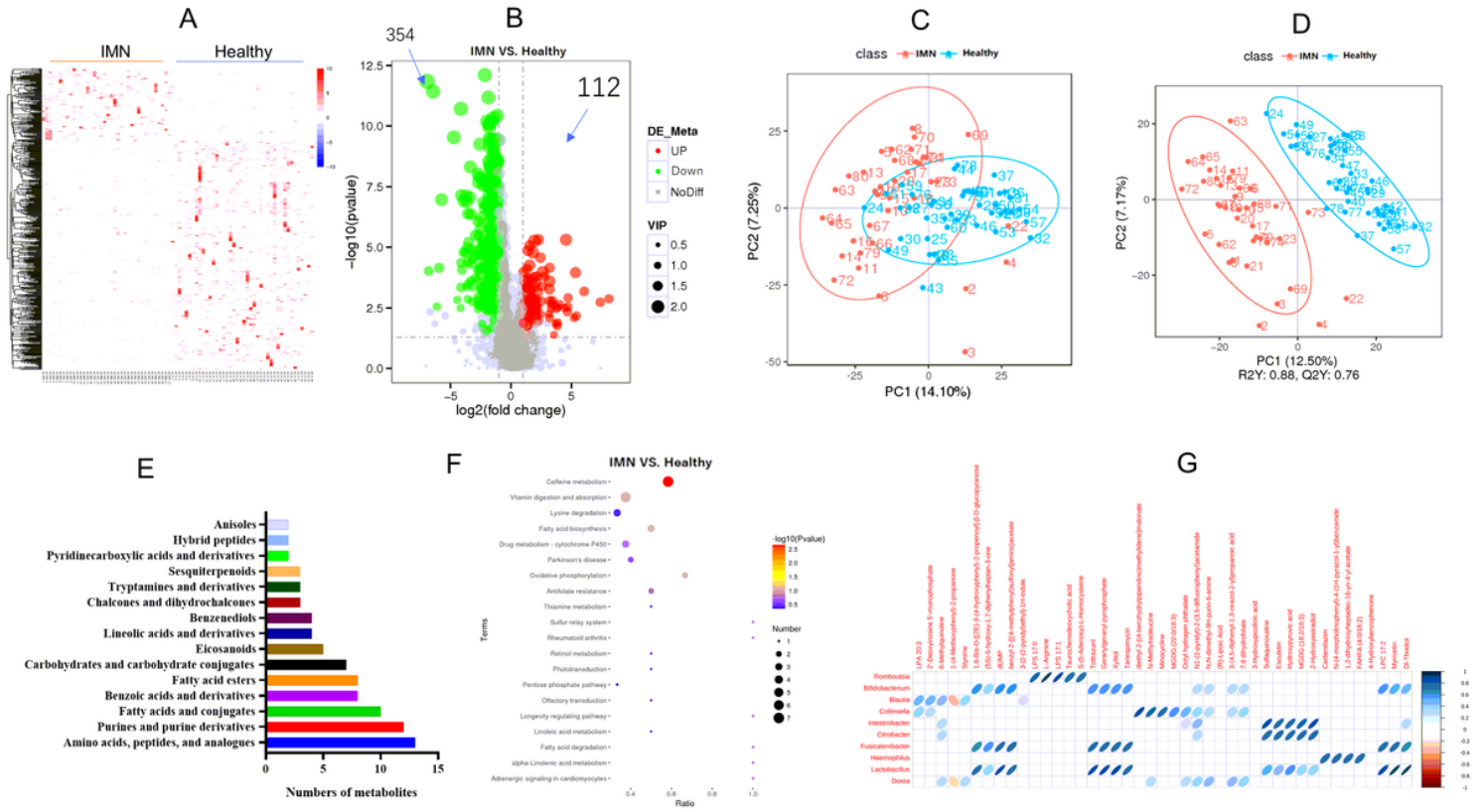

Figure 6

Fecal metabolite profiles of IMN patients and healthy control. A) Hierarchical cluster analysis. Columns represent fecal metabolite profiles of IMN patients and healthy controls. Red indicates increased abundance of individual metabolites relative to internal standard and blue indicates decreased abundance. B) volcano plots showing both P value and fold change of metabolites, with left being upregulated and right being down-regulated metabolites. C) PCA score plot of fecal metabolite profiles of IMN patients and healthy controls. D) PLS-DA score plot of fecal metabolite profiles of IMN patients and healthy controls. E) Chemical categories of differential metabolites; F) KEGG enrichment pathways based on differential metabolite; G) correlation analysis between top ten IMN enriched genus and differential metabolites.

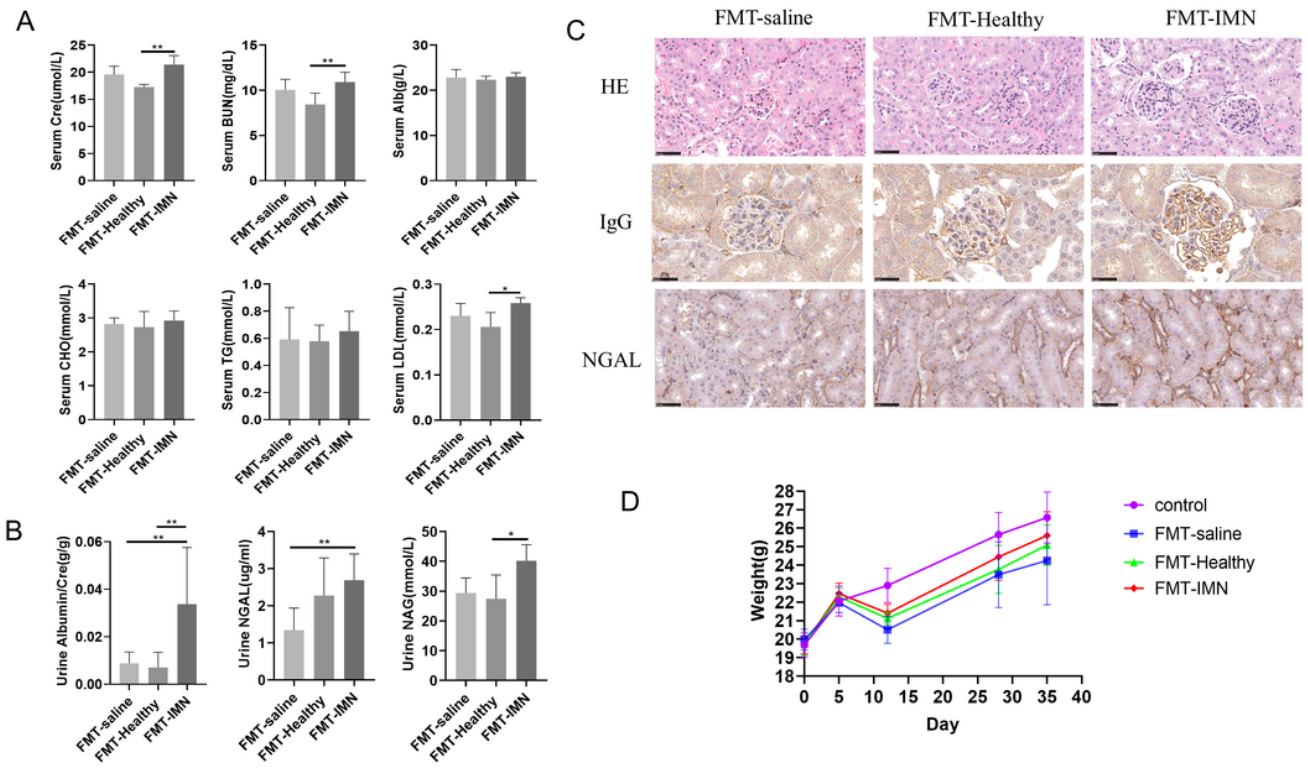

Figure 7

FMT transfer could cause decline of renal function and renal pathological injuries. Serum indexes among FMT-IMN, FMT-Healthy and FMT-saline; B) urine indexes among FMT-IMN, FMT-Healthy and FMT-saline; C) HE staining and immunohistochemistry to demonstrate that FMT with IMN feces can aggravate kidney impairment; D) Body weight dynamics of each groups.

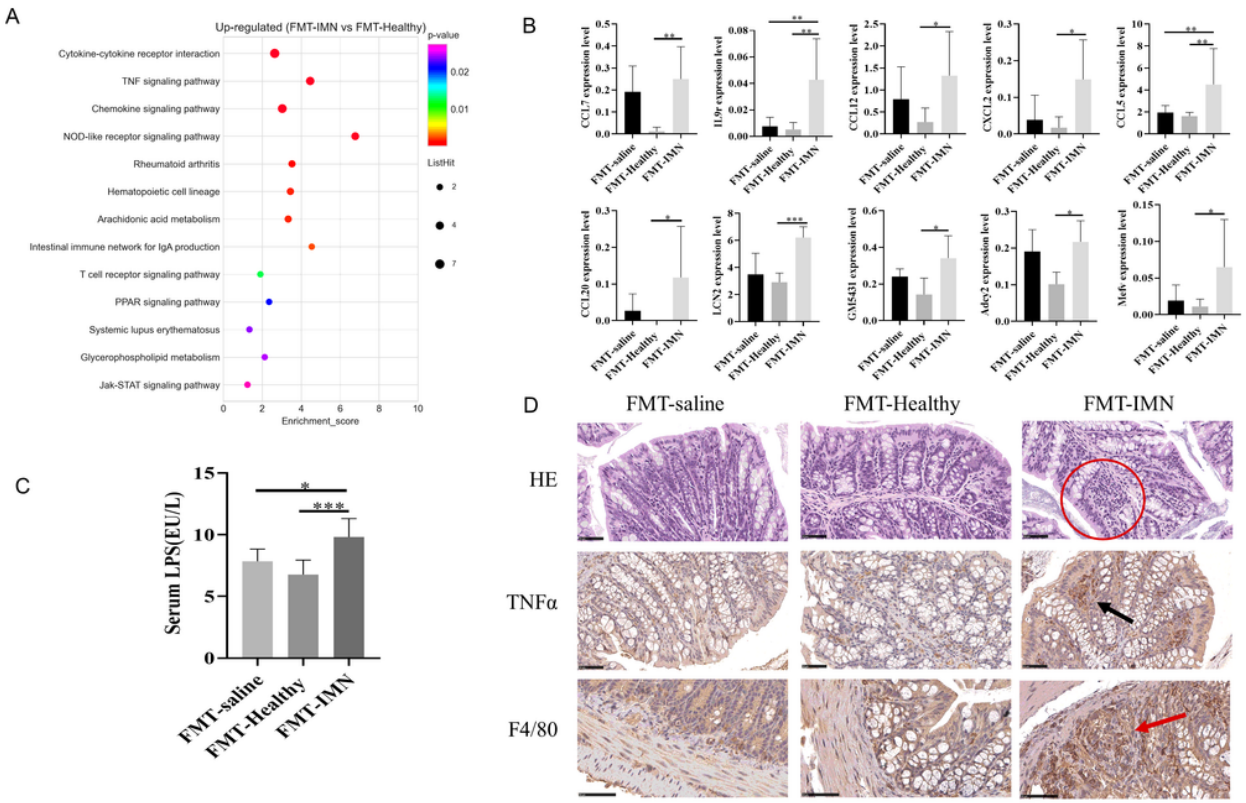

Figure 8

FMT transfer could cause decline due to intestinal inflammation, endotoxin and NOD-like receptor activation. A) KEGG pathway enrichment using mRNA sequencing data; B) QRT-PCR quantitation of mRNA sequencing results; C) serum LPS concentration tested by ELISA; D) HE staining and immunohistochemistry to demonstrate that FMT with IMN feces can aggravate intestinal impairment. Red cycle refers to inflammatory cells; black arrow refers to highly expressed TNFα cells, and red arrow indicates the F4/80 positive macrophages.

Supplementary Files

This is a list of supplementary files associated with this preprint. Click to download.

- supplementalfigS1.pptx
- TableS1.xlsx
- TableS2.xlsx
- figS3.pptx
- supplementalfigS2.jpg
- tableS4.xlsx
- tables3.xlsx